RSC Advances

PAPER

View Article Online
View Journal | View Issue

Cite this: *RSC Adv.*, 2016, **6**, 39074

Efficient polymer solar cells processed by environmentally friendly halogen-free solvents†

Zhe Zhang, Xuejuan Zhang, Jicheng Zhang, Xue Gong, Yahui Liu, Heng Lu, Cuihong Li* and Zhishan Bo*

Received 23rd February 2016
Accepted 12th April 2016

DOI: 10.1039/c6ra04835h

www.rsc.org/advances

The use of environmentally friendly halogen-free organic solvents for the fabrication of polymer solar cells will be of great importance for future practical applications. In this work, a new alternative conjugated polymer with 3,4-bis(octyloxy)-phenyl substituted benzo[1,2-*b*:4,5-*b*]dithiophene as the donor unit and benzo[*c*][1,2,5]thiadiazole as the acceptor unit was synthesized and used as the donor material for polymer solar cells. This polymer showed good solubility in halogen-free solvents such as toluene, *o*-xylene and so on. The blend film morphology, charge mobility and photovoltaic performance were investigated in halogen-free solvents. The photovoltaic devices fabricated from *o*-xylene with *N*-methyl-2-pyrrolidone as additive provided the best power conversion efficiency of 4.57%, comparable to that fabricated from halogenated solvents such as 1,2-dichlorobenzene/1,8-diiodooctane with a power conversion efficiency of 4.33%. Our results demonstrate that halogen-free solvents are promising for the fabrication of high efficiency polymer solar cells.

Introduction

Bulk heterojunction (BHJ) organic solar cells (OSCs) have experienced rapid progress in the past decade and a power conversion efficiency (PCE) higher than 9% has been achieved for both single junction and tandem OSCs.[1–11] The main advantage of OSCs is that they can be fabricated by low cost solution processing technology.[12–18] The most frequently used solvents for the fabrication of OSCs are halogenated organic solvents such as chlorobenzene (CB) and *o*-dichlorobenzene (DCB) that possess high boiling points, adequate viscosity, and superior solubility for nonpolar conjugated oligomers/polymers and fullerene derivatives. Unfortunately, these halogenated solvents are detrimental to human health and the environment, thus their use should be carefully considered from the view-points of large-scale roll-to-roll production and practical application.[19–21] Increasing attention has been paid to the use of halogen-free organic solvents, such as toluene, *o*-xylene, 1,2,4-trimethylbenzene, 1,2-dimethylnaphalene, anisole and so on, to replace halogenated ones for fabricating PSCs devices.[22–34] For example, Jen *et al.* used toluene solvents to fabricate devices based on **PIDII-DFBT** : $PC_{71}BM$ blends and PCE of 7.26% has been achieved. Li *et al.* fabricated the devices based **P3HT** : ICBA blend by halogen-free solvents and achieved a comparable PCE that is similar to the devices prepared from DCB. Hou *et al.* modified conjugated polymers and fullerene derivatives by triethylene glycol monoether functional group and a PCE of 5.23% was obtained by processing the active layer with halogen-free solvents. Wang *et al.* attached a polar and inert phosphonate moiety to the side chain of conventional photovoltaic polymers and a PCE of 2.11% was achieved by using anisole as the processing solvent. It is still challenging to fabricate PSCs using halogen-free organic solvents to achieve efficiency as high as that fabricated using halogenated solvents. Nevertheless, the use of environmentally friendly halogen-free organic solvents for the fabrication of PSCs will be of great importance for future practical applications.

Non-halogenated organic solvents, such as toluene, *o*-xylene and so on are biodegradable that produce little negative effect on environment and human health. In comparison with halogenated organic solvents, halogen-free organic solvents are usually poor solvents for fullerene derivatives such as $PC_{71}BM$. When halogen-free organic solvents were used as processing solvent, during the drying of active layer fullerene derivatives will first precipitate to form large aggregates, leading to unfavorable morphology and low efficiency.[35–37] It is possible to adjust the solubility of $PC_{71}BM$ in halogen-free organic solvents by using the additive. *N*-Methyl-2-pyrrolidone (NMP), which has a boiling point of 202 °C and is a good solvent for $PC_{71}BM$ (48 mg mL^{-1}), can be used as additive for halogen-free organic solvents to tune the morphology of active layer.[38] In addition, NMP is minimally flammable, of low toxicity and environmentally friendly. Encouraged by these ideas, we designed and

---

Beijing Key Laboratory of Energy Conversion and Storage Materials, College of Chemistry, Beijing Normal University, Beijing 100875, China. E-mail: licuihong@bnu.edu.cn; zsbo@bnu.edu.cn

† Electronic supplementary information (ESI) available: Experimental part including TGA curves, DSC curves, XRD curves, SCLC curves, and ^1H NMR and ^{13}C NMR spectra of monomers and ^1H NMR spectra of polymers. See DOI: 10.1039/c6ra04835h

synthesized bis(alkoxy)phenyl substituted benzo[1,2-*b*:4,5-*b*] dithiophene (BDT) based polymers (**PBBDTBT**), since BDT based polymers have been proved to be excellent donor materials.[5,11,39,40] The chemical structure of **PBBDTBT** is shown in Scheme 1. As expected, **PBBDTBT** showed a good solubility in halogen-free organic solvents such as toluene and *o*-xylene. After the addition of NMP as additive, the solubility of **PBBDTBT** in the solvent mixture decreased, leading to proper phase separation for the blend films and enhanced photovoltaic performance for the devices. The initial test revealed that the photovoltaic performance of **PBBDTBT** : $PC_{71}BM$ based devices fabricated with *o*-xylene/NMP as the processing solvent produced a PCE of 4.57%, higher than the PCE of 4.33% for devices fabricated from halogenated solvents (DCB/DIO).

Results and discussion

Material synthesis and characterization

Synthetic routes for the monomer and polymer are shown in Scheme 1. Compound **1**,[41] **2** [42] and **5** [43,44] were synthesized according to the literature procedure. The treatment of compound **2** with *n*-BuLi by lithium halogen exchange reaction afforded lithium intermediate, which was quenched with commercially available benzo[1,2-*b*:4,5-*b*′]dithiophene-4,8-dione to afford the intermediate diol. The diol was converted to compound **3** in a yield of 85% by the reaction with $SnCl_2\cdot 2H_2O$ in dilute hydrochloride acid. Abstraction of the two active hydrogen atoms of compound **3** by *n*-BuLi was followed by reaction with trimethyltin chloride to furnish monomer **4** in a yield of 87%. Stille polycondensation of monomer **4** and compound **5** afforded copolymer **PBBDTBT** as a black-blue solid. The number average molecular weights (M_n) and polydispersity (PDI) of **PBBDTBT** were determined by gel permeation chromatography (GPC) using THF as an eluent and narrowly distributed polystyrenes as calibration standards to be 43 kg mol^{-1} and 3.0, respectively. The related data are summarized in Table 1. **PBBDTBT** was fully soluble in common organic solvents such as dichloromethane (DCM), chloroform (CF), *o*-xylene and DCB at room temperature, and could be fully dissolved in toluene at about 50 °C. Thermogravimetric analysis (TGA) and differential scanning calorimetry (DSC) experiments were carried out under nitrogen atmosphere at a heating rate of 10 °C min^{-1} to investigate thermal properties of **PBBDTBT**. As shown in Fig. S3 and S4,† the TGA curve demonstrated that **PBBDTBT** is of good thermal stability with a 5% decomposition temperature up to 333 °C. DSC measurement showed no obvious glass transition in the range of 60 to 250 °C, reflecting **PBBDTBT** could be amorphous. X-ray diffraction (XRD) experiments were carried out to investigate the packing properties of **PBBDTBT** in the solid state. As shown in Fig. S5,† **PBBDTBT** presents two diffraction peaks, the first peak at 3.67° in the small angle region could be ascribed to the distance between polymer chains separated by flexible side chains and the second broad peak centered at 22.55° in the wide angle region could be ascribed to the π–π stacking distance of polymer backbones. According to the Bragg equation, these distances were calculated to be 24.09 and 3.91 Å, respectively. Such a broad diffraction peak in the wide angle region indicated that this polymer is amorphous.

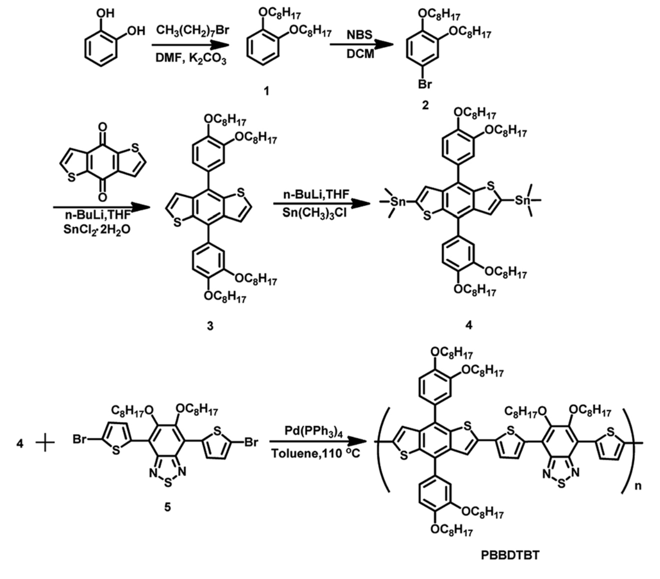

Scheme 1 Synthetic routes for PBBDTBT.

Optical and electrochemical properties

UV-vis absorption characteristics of **PBBDTBT** were investigated in different solvents such as toluene, *o*-xylene and DCB (1×10^{-5} M) at room temperature and as films. As shown in Fig. 1, in toluene, *o*-xylene and DCB solutions **PBBDTBT** exhibited similar absorption spectra with a weak absorption peak at 419 nm and an intense absorption peak at 574 nm and a should peak at about 612 nm, with a molar extinction coefficient of 50.34 L g^{-1} cm^{-1} in *o*-xylene. The first peak at 419 nm could be ascribed to the π–π* transition and the second peak and the shoulder could be attributed to the intramolecular charge transfer interaction (ICT) between BDT unit and benzo-2,1,3-thiadiazole unit.[7] In going from solution to film, **PBBDTBT** displayed a broader spectrum with two red-shifted peaks at 433 and 590 nm and a shoulder peak at 625 nm, indicating the formation of ordered stacking in some extent as films. The absorption data are also summarized in Table 1. The optical band gap ($E_{g,opt}$) of **PBBDTBT** was evaluated from the film absorption onset to be 1.76 eV. Upon blending with $PC_{71}BM$, films spin coated from toluene and *o*-xylene solutions revealed similar absorption properties; whereas films spin coated from DCB solutions exhibited a slightly broad absorption peak with the shoulder peak at 630 nm became more intense, indicating that polymer chains could form more ordered packing when spin coated from DCB solutions. The absorption valley of polymers in the short wavelength region was compensated by the absorption of $PC_{71}BM$.

Electrochemical properties of **PBBDTBT** were investigated by cyclic voltammetry (CV) with a standard three-electrode electrochemical cell. As shown in Fig. 2, the oxidation onset of **PBBDTBT** film was determined to be 0.72 V and the HOMO level

Table 1 Physical, electronic, and optical properties of **PBBDTBT**

Polymer	$T_d{}^a$ (°C)	λ (nm) solution	λ (nm) film	$E_{g,opt}{}^b$ (eV)	HOMO (eV)	LUMO (eV)
PBBDTBT	333	419, 574	433, 590, 627	1.76	−5.43	−3.67

[a] T_d is the 5% weight-loss temperature under N_2 atmosphere. [b] Calculated from the onset absorption of **PBBDTBT**, $E_{g,opt} = 1240/\lambda_{onset}$.

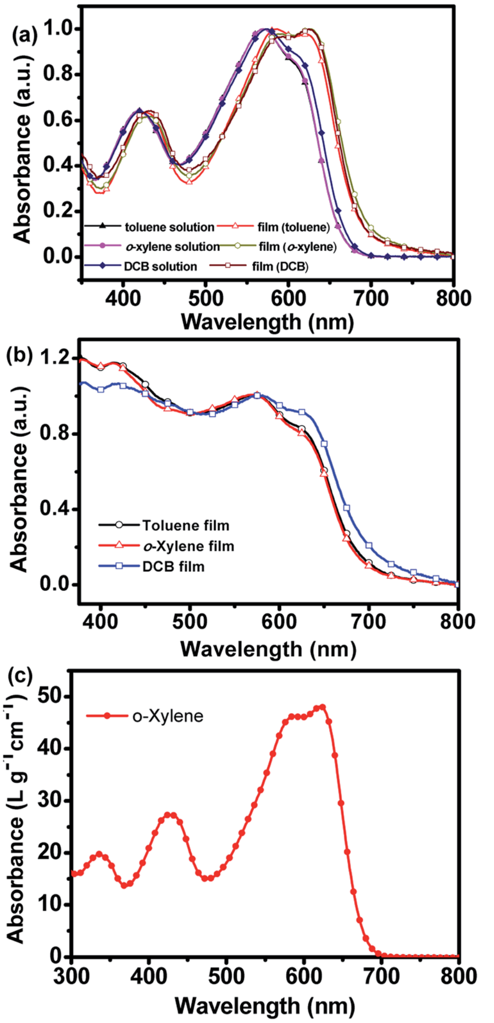

Fig. 1 UV-vis absorption spectra of (a) **PBBDTBT** in diluted toluene, *o*-xylene and DCB solutions and as films; (b) **PBBDTBT** : $PC_{71}BM$ (1 : 1.5 by weight) blending films spin coated from toluene, *o*-xylene and DCB solutions; (c) molar extinction coefficient of **PBBDTBT** in diluted *o*-xylene.

of **PBBDTBT** was calculated to be −5.43 eV using the equation: $E_{HOMO} = -e(E_{ox} + 4.71)$ (eV). The LUMO level was calculated to be −3.67 eV according to the equation $E_{LUMO} = E_{HOMO} + E_{g,opt}$. The results are also summarized in Table 2.

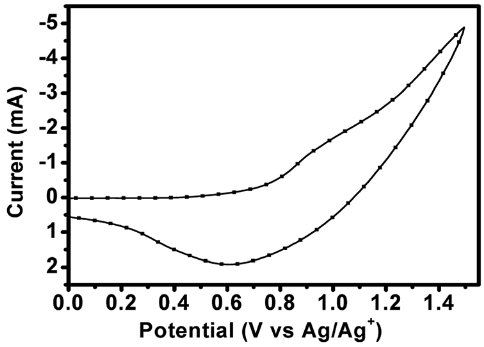

Fig. 2 Cyclic voltammogram of **PBBDTBT** as films on a platinum electrode in 0.1 mol L^{-1} Bu_4NPF_6 acetonitrile solution at a scan rate of 100 mV s^{-1}.

Photovoltaic properties

A conventional device structure of ITO/PEDOT : PSS/**PBBDTBT** : $PC_{71}BM$/LiF/Al was adopted to investigate the photovoltaic performance of **PBBDTBT** : $PC_{71}BM$ based PSCs fabricated from halogen-free solvents such toluene and *o*-xylene. Devices fabricated from DCB solutions were also tested for a comparison. All devices with varied D/A ratios exhibited in Table S1,† and the best photovoltaic performance in a donor/acceptor weight ratio of 1 : 1.5. *J*–*V* curves of optimized devices measured under simulated solar illumination (AM1.5G, 100 mW cm^{-2}) are shown in Fig. 3a and the device parameters are summarized in Table 2. For plain devices fabricated with toluene and *o*-xylene as the processing solvents, inferior PCEs of 0.73% and 1.35% were achieved; whereas a PCE of 3.22% was obtained using DCB as the processing solvent. The different photovoltaic performance might be due to the inferior solubility of $PC_{71}BM$ in toluene or *o*-xylene to DCB. The boiling point and evaporation speed of processing solvent have a significant influence on the morphology of blend films. Active layers spin-coated from toluene and *o*-xylene solutions exhibited a severe phase separation with larger spherical grains.[30] The unfavorable film morphology is responsible for the poor photovoltaic performance of devices fabricated with toluene or *o*-xylene as the processing solvent. To tune the morphology of blend films different additives were utilized. When 3% NMP (by volume) was used as additive in the toluene solution, an improved PCE of 2.10% with V_{oc} of 0.71 V, J_{sc} of 5.80 mA cm^{-2} and FF of 0.51 was achieved. Similarly, higher PCE of 4.57% with V_{oc} of 0.73 V, J_{sc} of 8.94 mA cm^{-2} and FF of 0.70 was obtained for devices fabricated from *o*-xylene with 4% NMP (by volume) as additive. The increased J_{sc} and FF contributed to the overall enhanced photovoltaic performance. In contrast, when DCB containing 3% DIO (by volume) was used as the processing solvent, a PCE of 4.33% was achieved. Notably, optimized devices fabricated from *o*-xylene/NMP solutions showed superior performance to that fabricated from DCB/DIO solutions, demonstrating that halogen-free solvent *o*-xylene is promising for future commercial application.

Table 2 Summary of the photovoltaic properties of the solar cells

Solvent	Solvent additive	V_{oc} (V)	J_{sc} (mA cm^{-2})	FF	PCE (%) best/ave[a]	d (nm)	Hole mobility (cm^2 V^{-1} s^{-1})
Toluene	No	0.77	2.77	0.34	0.73/0.61	194	4.15×10^{-6}
	3% NMP	0.71	5.80	0.51	2.10/1.96	171	1.05×10^{-5}
o-Xylene	No	0.78	3.86	0.45	1.35/1.24	128	8.73×10^{-6}
	4% NMP	0.73	8.94	0.70	4.57/4.50	138	1.48×10^{-5}
DCB	No	0.76	6.62	0.64	3.22/3.11	124	1.18×10^{-5}
	3% DIO	0.71	8.97	0.68	4.33/4.25	137	1.52×10^{-5}

[a] The average PCEs were based on ten devices.

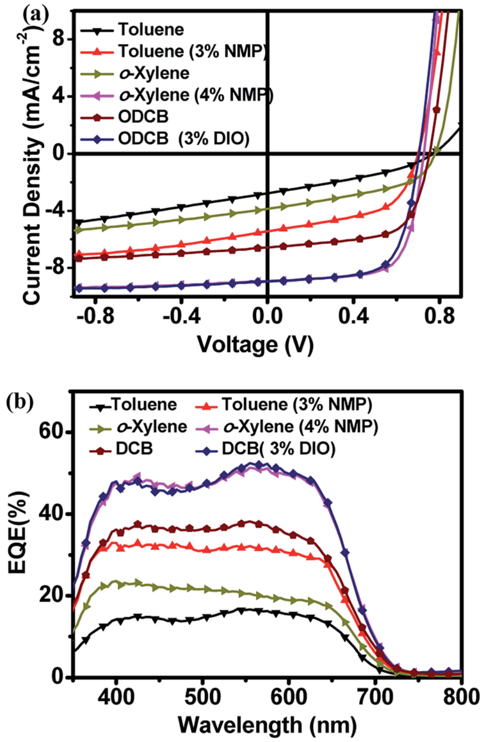

Fig. 3 (a) The J–V characteristics of devices based on **PBBDTBT** : PC$_{71}$BM under the illumination of AM1.5G (100 mW cm^{-2}); (b) EQE curves of solar cells fabricated under different conditions.

External quantum efficiencies (EQEs) were measured to examine the accuracy of J_{sc} from the J–V measurements. As shown in Fig. 3b, EQE spectra of the devices processed by toluene, *o*-xylene, and DCB are in the range of 350 to 700 nm. The results demonstrated that devices fabricated with additives have higher EQE values than that fabricated without using additives, indicating the use of additive is favorable to form appropriate morphology for charge separation and transport. The J_{sc} calculated from the integration of EQE curves agreed well with that obtained from J–V measurement, verifying the accuracy of the PCE obtained from J–V measurements.

Hole and electron mobilities

Hole mobilities of blend films were measured with space charge limited current (SCLC) method and the results are summarized in Table 2. Devices were fabricated from different solvents with a typical structure of ITO/PEDOT : PSS/**PBBDTBT** : PC$_{71}$BM (1 : 1.5 w/w)/Au. Electron mobilities of blend films were measured and the results are summarized in Table S2.† Devices were fabricated from different solvents with a typical structure of FTO/**PBBDTBT** : PC$_{71}$BM (1 : 1.5 w/w)/Al. Dark J–V experiments were carried out and the hole mobility of **PBBDTBT** was calculated from $J = 9\varepsilon_0\varepsilon_r\mu V^2/8L^3$. The curves are shown in Fig. S6 and S7.† **PBBDTBT** : PC$_{71}$BM based plain devices fabricated from toluene, *o*-xylene and DCB exhibited hole mobilities of 4.15×10^{-6}, 8.73×10^{-6}, and 1.18×10^{-5} cm^2 V^{-1} s^{-1}, respectively. Hole mobilities were improved to 1.05×10^{-5}, 1.48×10^{-5}, 1.52×10^{-5} cm^2 V^{-1} s^{-1} for devices fabricated from toluene containing 3% NMP, *o*-xylene containing 4% NMP, and DCB containing 3% DIO, respectively. The improvement of hole mobilities, which matched better the electron mobility, could be ascribed to the optimization of film morphology after using solvent additive. More balanced charge mobility is beneficial for the charge transport in the devices, leading to higher J_{sc} and FF.

The blend film morphology

The morphology of the active layer has an obvious influence on the photovoltaic performance of devices. Therefore, atomic force microscopy (AFM) was used to investigate the morphology of blend films spin coated from different solvents. As shown in Fig. 4, the blend films spin coated from toluene and *o*-xylene solutions exhibited a relatively rough surface topography with large spherical aggregates and the root-mean-square (R_a) values are 16.6 and 12.0 nm, respectively. Such high roughness values can be attributed to low solubility of PC$_{71}$BM in toluene and *o*-xylene. Interestingly, after NMP was used as the additive in toluene and *o*-xylene, the blend films showed distinct differences in morphologies from the system without NMP. Both films became smooth, and the roughness values were decreased to be 9.29 and 3.53 nm, respectively. The solubility of conjugated polymers and PC$_{71}$BM has a significant influence on the morphology of blend films. **PBBDTBT** exhibited a good solubility in toluene, *o*-xylene and DCB; whereas the solubility of PC$_{71}$BM in toluene and *o*-xylene is poorer than that in DCB. When toluene or *o*-xylene is used as the processing solvent, PC$_{71}$BM will firstly precipitate from the solution to form large aggregates during drying of the active layer. After adding NMP, the solubility of polymer in blend solutions will decrease, leading to the formation of polymer networks, which can

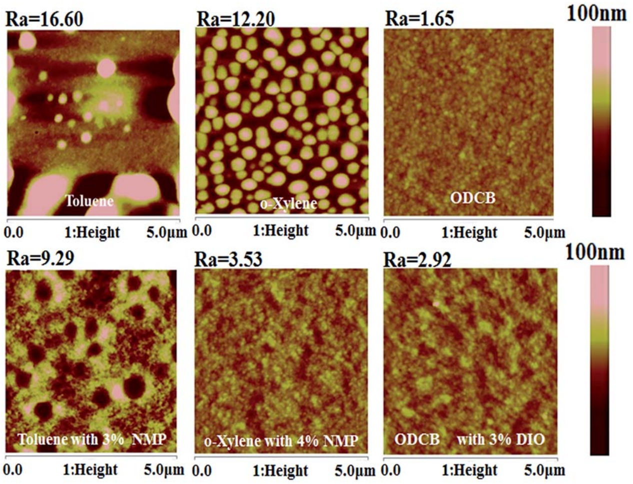

Fig. 4 AFM height images of **PBBDTBT** : $PC_{71}BM$ (1 : 1.5, w/w) blend films spin-coated from different solvents.

prevent the formation of large spherical $PC_{71}BM$ aggregates during the drying of blend films. As for blend films spin-coated from DCB solutions, the morphology became rougher and the R_a value increased from 1.65 to 2.29 nm after using DIO as additive. Obviously, the addition of a small amount of polar solvent as the additive to non-halogenated solvents such as toluene and *o*-xylene can significantly promote micro-phase separation for the blend films and have a profound effect on the photovoltaic performance.

Conclusions

3,4-Bis(octyloxy)-phenyl substituted benzo[1,2-*b*:4,5-*b*]dithiophene (BDT) based polymer (**PBBDTBT**) was designed and synthesized. **PBBDTBT** showed a good solubility in halogen-free solvents such as toluene, *o*-xylene and so on. The influence of non-halogenated solvent on the morphology, charge mobility and photovoltaic performance was thoroughly investigated. **PBBDTBT** : $PC_{71}BM$ based PSCs processed from non-halogenated solvent *o*-xylene/NMP produced the best PCE of 4.57% with a V_{oc} of 0.73 V, a J_{sc} of 8.94 mA cm^{-2} and an FF of 0.70, higher than the devices fabricated using halogenated solvents such as DCB/DIO with a PCE of 4.33%. Our results have demonstrated that non-halogenated solvents are promising for the fabrication of high efficiency PSCs.

Experimental part

4,8-Bis(1,2-bis(octyloxy)-4-phenyl)-benzo[1,2-*b*:4,5-*b*′]-dithiophene (3)

Under protection of nitrogen, 2.4 M *n*-butyllithium (*n*-BuLi) solution in *n*-hexane (3.05 mL) was slowly added to 4-bromo-1,2-bis(octyloxy)benzene (3 g, 7.25 mmol) in THF (50 mL) at −78 °C, and the mixture was kept at −78 °C for 1 h. Benzo[1,2-*b*:4,5-*b*′]dithiophene-4,8-dione (0.76 g, 3.45 mmol) was added, and the mixture was stirred overnight at the room temperature. Then $SnCl_2 \cdot 2H_2O$ (1.8 g) in 20% HCl (25 mL) was added and the mixture was stirred for 5 h at the room temperature. The mixture was poured into ice water and extracted by dichloromethane (DCM) three times. The combined organic phase was dried over magnesium sulfate and evaporated to afford the crude product. Further purification was carried out on a silica gel column, eluting with pure petroleum ether. White crystals were obtained (1.92 g, 65%). ^1H NMR (400 MHz, $CDCl_3$): δ 7.58 (d, $J = 5.6$ Hz, 1H), δ 7.50 (s, 2H), δ 7.09 (d, $J = 5.6$ Hz, 1H), δ 7.00 (d, $J = 8.6$ Hz, 1H), δ 3.97–3.92 (m, 4H), δ 1.89–0.99 (m, 30H). ^{13}C NMR (100 MHz, $CDCl_3$): δ 149.11, 148.99, 138.23, 136.13, 131.92, 130.21, 127.11, 123.18, 121.86, 114.91, 113.67, 69.28, 31.87, 31.84, 29.45, 29.42, 29.33, 29.29, 26.13, 26.05, 22.71, 22.69, 14.13. Anal. calcd for $C_{54}H_{78}O_4S_2$: C 75.83; H 9.19. Found: C 75.87; H 9.52.

4,8-Bis(1,2-bis(octyloxy)-4-phenyl)-benzo[1,2-*b*:4,5-*b*′]-dithiophene-2,6-bis(trimethyltin) (4)

To a solution of compound 3 (0.5 g, 0.585 mmol) in THF (40 mL) at −78 °C was slowly added 2.4 M *n*-butyllithium solution in *n*-hexane (0.61 mL). After the addition, the solution was warmed slowly to room temperature and kept for 1 h. After cooling down to the −78 °C, 1.0 M trimethyltin chloride solution in THF (1.29 mL) was added. The mixture was stirred overnight at the room temperature and quenched with water. The mixture was extracted with diethyl ether three times and dried by over $MgSO_4$, the solvent was removed and the residue was recrystallized from hexane to afford the compound 4 (0.62 g, 90%). ^1H NMR (400 MHz, $CDCl_3$): δ 8.04 (s, 1H), δ 7.70–7.68 (m, 2H), δ 7.04 (d, $J = 8.04$ Hz, 1H), δ 4.00–3.93 (m, 4H), δ 1.84–1.01 (m, 30H). δ 0.39–0.25 (m, 9H). ^{13}C NMR (100 MHz, $CDCl_3$): δ 148.93, 148.78, 142.47, 141.78, 136.99, 132.53, 131.00, 128.64, 121.80, 115.08, 113.51, 69.23, 69.18, 31.87, 31.84, 29.46, 29.42, 29.33, 29.32, 29.26, 26.15, 26.07, 22.72, 22.69, 14.14, 14.12. Anal. calcd for $C_{60}H_{94}O_4S_2Sn_2$: C 61.02; H 8.02. Found: C 61.07; H 7.86.

PBBDTBT

4 (120 mg, 0.1016 mmol) and **5** (72.62 mg, 0.1016 mmol) were dissolved in toluene (5 mL) and DMF (1 mL) in a 50 mL double-neck round-bottom flask. The reaction container was carefully degassed before and after the addition of $Pd(PPh_3)_4$ (5.0 mg, 4.32 μmol). The mixture was stirred and refluxed under nitrogen atmosphere for 24 h. Then the mixture was cooled to room temperature and poured into methanol (150 mL), the precipitates was subjected to Soxhlet extraction with methanol, hexane and DCM. The polymer was recovered as a solid from the DCM fraction by natural sedimentation from methanol. Polymers were obtained as black-blue solid (106.5 mg, 73%). GPC (PS standards): $M_n = 43$ kg mol^{-1}, $M_w = 130$ kg mol^{-1} and PDI = 3.0.

Acknowledgements

Financial support from the NSF of China (51003006, 21161160443), the 973 Programs (2011CB935702), Beijing Natural Science Foundation (2132042), Program for Changjiang Scholars and Innovative Research Team in University and the

Fundamental Research Funds for the Central Universities are gratefully acknowledged.

References

1 J. D. Chen, C. H. Cui, Y. Q. Li, L. Zhou, Q. D. Ou, C. Li, Y. F. Li and J. X. Tang, *Adv. Mater.*, 2015, **27**, 1035.

2 J. B. You, L. T. Dou, K. Yoshimura, T. Kato, K. Ohya, T. Moriarty, K. Emery, C. C. Chen, J. Gao, G. Li and Y. Yang, *Nat. Commun.*, 2013, **4**, 1446.

3 C. C. Chen, W. H. Chang, K. Yoshimura, K. Ohya, J. You, J. Gao, Z. Hong and Y. Yang, *Adv. Mater.*, 2014, **26**, 5670.

4 S. Roland, S. Neubert, S. Albrecht, B. Stannowski, M. Seger, A. Facchetti, R. Schlatmann, B. Rech and D. Neher, *Adv. Mater.*, 2015, **27**, 1262.

5 Z. C. He, B. Xiao, F. Liu, H. B. Wu, Y. Yang, S. Xiao, C. Wang, T. P. Russell and Y. Cao, *Nat. Photonics*, 2015, **9**, 174.

6 H. Q. Zhou, Y. Zhang, C. K. Mai, S. D. Collins, G. C. Bazan, T. Q. Nguyen and A. J. Heeger, *Adv. Mater.*, 2015, **27**, 1767.

7 J. C. Zhang, G. W. Li, C. Kang, H. Lu, X. X. Zhao, C. H. Li, W. H. Li and Z. S. Bo, *Dyes Pigm.*, 2015, **115**, 181.

8 Y. H. Liu, J. B. Zhao, Z. K. Li, C. Mu, W. Ma, H. W. Hu, K. Jiang, H. R. Lin, H. Ade and H. Yan, *Nat. Commun.*, 2014, **5**, 5293.

9 W. C. Zhao, L. Ye, S. Q. Zhang, B. Fan, M. L. Sun and J. H. Hou, *Sci. Rep.*, 2014, **4**, 6570.

10 W. C. Zhao, L. Ye, S. Q. Zhang, H. F. Yao, M. L. Sun and J. H. Hou, *J. Phys. Chem. C*, 2015, **119**, 27322.

11 K. Q. Zhao, X. Y. Bai, B. Xiao, Y. Gao, P. Hu, B. Q. Wang, Q. D. Zeng, C. Wang, B. Heinrichc and B. Donnio, *J. Mater. Chem. C*, 2015, **3**, 11735.

12 R. Søndergaard, M. Hösel, D. Angmo, T. T. Larsen-Olsen and F. C. Krebs, *Mater. Today*, 2012, **15**, 36.

13 Y. J. Kim, Y. R. Cheon, J. W. Jang, Y. H. Kim and C. E. Park, *J. Mater. Chem. C*, 2015, **3**, 1904.

14 S. Günes, H. Neugebauer and N. S. Sariciftci, *Chem. Rev.*, 2007, **107**, 1324.

15 L. Fan, R. L. Cui, X. P. Guo, D. Qian, B. B. Qiu, J. Yuan, Y. F. Li, W. L. Huang, J. L. Yang, W. F. Liu, X. J. Xu, L. D. Li and Y. P. Zou, *J. Mater. Chem. C*, 2014, **2**, 5651.

16 Y. F. Li, *Acc. Chem. Res.*, 2012, **45**, 723.

17 J. W. Chen and Y. Cao, *Acc. Chem. Res.*, 2009, **42**, 1709.

18 Z. Lu, C. H. Li, C. Du, X. Gong and Z. S. Bo, *Chin. J. Polym. Sci.*, 2013, **31**, 901.

19 P. G. Jessop, *Green Chem.*, 2011, **13**, 1391.

20 T. R. Andersen, T. T. Larsen-Olsen, B. Andreasen, A. P. Bottiger, J. E. Carle, M. Helgesen, E. Bundgaard, K. Norrman, J. W. Andreasen, M. Jørgensen and F. C. Krebs, *ACS Nano*, 2011, **5**, 4188.

21 C. C. Chueh, K. Yao, H. L. Yip, C. Y. Chang, Y. X. Xu, K. S. Chen, C. Z. Li, P. Liu, F. Huang, Y. W. Chen, W. C. Chen and A. K. Y. Jen, *Energy Environ. Sci.*, 2013, **6**, 3241.

22 K. S. Chen, H. L. Yip, C. W. Schlenker, D. S. Ginger and A. K. Y. Jen, *Org. Electron.*, 2012, **13**, 2870.

23 B. R. Aïch, S. Beaupré, M. Leclerc and Y. Tao, *Org. Electron.*, 2014, **15**, 543.

24 P. T. Tsai, C. Y. Tsai, C. M. Wang, Y. F. Chang, H. F. Meng, Z. K. Chen, H. W. Lin, H. W. Zan, S. F. Horng, Y. C. Lai and P. C. Yu, *Org. Electron.*, 2014, **15**, 893.

25 C. H. Duan, W. Z. Cai, B. B. Y. Hsu, C. M. Zhong, K. Zhang, C. C. Liu, Z. C. Hu, F. Huang, G. C. Bazan, A. J. Heeger and Y. Cao, *Energy Environ. Sci.*, 2013, **6**, 3022.

26 J. H. Chang, H. F. Wang, W. C. Lin, K. M. Chiang, K. C. Chen, W. C. Huang, Z. Y. Huang, H. F. Meng, R. M. Ho and H. W. Lin, *J. Mater. Chem. A*, 2014, **2**, 13398.

27 B. Meng, Y. Y. Fu, Z. Y. Xie, J. Liu and L. X. Wang, *Polym. Chem.*, 2015, **6**, 805.

28 Y. Chen, Y. Cui, S. Q. Zhang and J. H. Hou, *Polym. Chem.*, 2015, **6**, 4089.

29 W. C. Zhao, L. Ye, S. Q. Zhang, M. L. Sun and J. H. Hou, *J. Mater. Chem. A*, 2015, **3**, 12723.

30 Y. Chen, S. Q. Zhang, Y. Wu and J. H. Hou, *Adv. Mater.*, 2014, **26**, 2744.

31 Y. Zhang, J. Y. Zou, C. C. Cheuh, H. L. Yip and A. K. Y. Jen, *Macromolecules*, 2012, **45**, 5427.

32 X. Guo, M. J. Zhang, C. H. Cui, J. H. Hou and Y. F. Li, *ACS Appl. Mater. Interfaces*, 2014, **6**, 8190.

33 L. Ye, S. Q. Zhang, L. J. Huo, M. J. Zhang and J. H. Hou, *Acc. Chem. Res.*, 2014, **47**, 1595.

34 D. L. Liu, Z. Y. Wang, S. Q. Zhang, Z. Zheng, B. Yang, W. Ma and J. H. Hou, *RSC Adv.*, 2015, **5**, 69567.

35 K. R. Graham, P. M. Wieruszewski, R. Stalder, M. J. Hartel, J. G. Mei, F. So and J. R. Reynolds, *Adv. Funct. Mater.*, 2012, **22**, 4801.

36 Y. Yao, J. H. Hou, Z. Xu, G. Li and Y. Yang, *Adv. Funct. Mater.*, 2008, **18**, 1783.

37 F. Machui, S. Langner, X. D. Zhu, S. Abbott and C. J. Brabec, *Sol. Energy Mater. Sol. Cells*, 2012, **100**, 138.

38 J. K. Lee, W. L. Ma, C. J. Brabec, J. Yuen, J. S. Moon, J. Y. Kim, K. Lee, G. C. Bazan and A. J. Heeger, *J. Am. Chem. Soc.*, 2008, **130**, 3619.

39 D. Y. Liu, C. Y. Gu, M. J. Xiao, M. Qiu, M. L. Sun and R. Q. Yang, *Polym. Chem.*, 2015, **6**, 3398.

40 Q. Liu, X. C. Bao, L. L. Han, C. T. Gu, M. Qiu, Z. K. Du, R. Y. Sheng, M. L. Sun and R. Q. Yang, *Sol. Energy Mater. Sol. Cells*, 2015, **138**, 26.

41 E. Westphal, I. H. Bechtold and H. Gallardo, *Macromolecules*, 2010, **43**, 1319.

42 J. M. Murphy, X. B. Liao and J. F. Hartwig, *J. Am. Chem. Soc.*, 2007, **129**, 15434.

43 C. Zhou, Y. M. Liang, F. Liu, C. Sun, X. L. Huang, Z. Q. Xie, F. Huang, J. Roncali, T. P. Russell and Y. Cao, *Adv. Funct. Mater.*, 2014, **24**, 7538.

44 H. D. Wei, H. Lu, T. Fang and Z. S. Bo, *Sci. China: Chem.*, 2015, **58**, 286.